CI-Sentaurus: A Quantum-Poisson Self-Consistent Solution of a Quantum Dot

Erik Nielsen, Ralph Young, Malcolm Carroll, and Richard P. Muller

SAND2011-5805C

Quantum Information S&T

INTRODUCTION

Semiconductor devices having regions with few electrons, which need to be modeled quantum mechanically, and regions of high electron density, which should be treated semi-classically, are typical in the area of quantum computing. The MOS double quantum dots fabricated at Sandia exemplify this type of device. Simulation of such devices proves challenging because quantum and semi-classical solutions must be integrated in a way not anticipated by existing semiconductor design tools. As a result, we have worked to couple a commercially available semi-classical tool, Sentaurus Device, with a quantum-mechanical configuration interaction (CI) module. By carefully iterating between Sentaurus Device and the CI module, we are able to simulate advanced three dimensional device geometries which have a "quantum" sub-region containing a few electrons. The solution accounts for the redistribution of charge in the non-quantum region due to the quantum mechanical charge distribution in the quantum region.

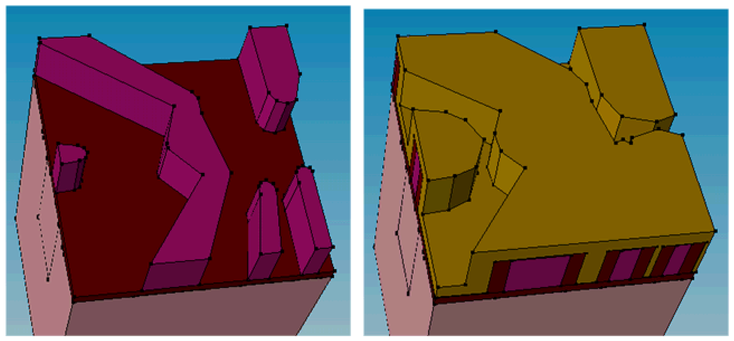

Figure 1. Left Side of Double Quantum Dot Structure showing Polysilicon Gates (left) covered by Al_2O_3 (right). A top metal accumulation gate (not shown) covers the Al_2O_3.

METHOD

Our method consists of a loop between a commercial finite volume package (Sentaurus Device) and a configuration interaction code. Sentaurus solves the nonlinear Poisson equation

$$\nabla^2\phi(\vec{r}) = N_c F\left(\frac{\phi(\vec{r}) - \Delta_{bgn}(\vec{r}) - E_F}{k_B T}\right) \quad (1)$$

where ϕ is the electrostatic potential (a constant shift from the conduction band edge E_C), E_F is the Fermi energy, T is the temperature, and k_B is the Boltzmann constant. Δ_{bgn} is a band gap narrowing term used to account for dopant-dependent changes in a material's band gap. In addition to the electrostatic potential ϕ, solving Eq. 1 also gives the electron density as a function of space, $n(\vec{r})$. In this usage Sentaurus Device invokes no quantum mechanical effects.

The full configuration interaction technique diagonalizes a many-particle Hamiltonian in a specified basis, giving the energies and eigenfunctions of the quantum system. The general form the Hamiltonian we consider is

$$\mathcal{H} = \sum_i^n \frac{\left(\vec{p}_i - e\vec{A}\right)^2}{2m^*} + \phi(\vec{r}_i) + g\mu_B \vec{S}_i \cdot \vec{B} + \sum_{i<j} \frac{e^2}{\kappa\left|\vec{r}_i - \vec{r}_j\right|} \quad (2)$$

where $\vec{r}_i$ and $\vec{p}_i$ are the position and momentum, respectively, of the i^{th} electron, ϕ is the electrostatic potential, and m^* is the effective mass (generally a tensor). A vector potential $\vec{A}$ determines the magnetic field $\vec{B} = \nabla \times \vec{A}$, which we restrict to be constant and along the *z*-direction: $\vec{B} = B\hat{z}$, and κ is an effective dielectric constant. The specific implementation we have developed uses a basis of non-orthogonal *s*-type Gaussian functions, centered at different spatial locations, to construct a set of orthogonal single-particle functions. Multi-particle slater determinant functions are formed from this orthogonal set, and the Hamiltonian (Eq. 2) is diagonalized in this basis using sparse matrix routines when necessary.

Hamiltonian (Eq. 2) is diagonalized in this basis using sparse matrix routines when necessary.

The loop between Sentaurus and the CI module is structured as follows:

1. Sentaurus is used to optimize the gate control voltages so that there are N electrons in a pre-defined "quantum region" of space.
2. Sentaurus exports the electrostatic potential and electron density (as a function of space) within the quantum region and sends to CI preprocessor.
3. CI preprocessor subtracts from the supplied electrostatic potential the potential due to the supplied electron charge density. The result is the electrostatic potential in the quantum region due only to charges outside the region.
4. CI preprocessor finds the minimum (or minima) in the electrostatic potential resulting from the last step. Along the *z*-direction at each minimum, a linear fit potential gives a 1D triangular well approximation. The ground state of a triangular well is given by an Airy function. A 1D Gaussian is centered at the peak of this Airy function and its width is determined by optimizing its overlap with the Airy function. The width and location of this 1D Gaussian are used as the *z*-dependent parts of all of the Gaussian basis functions in the next step. At the *z*-value where the Airy function peaks, parabolic fits to the potential along the *x* and *y* directions determine the *x* and *y* widths of the Gaussian basis functions.
5. CI obtains the energies and eigenstates of electrons within the quantum region using a Gaussian basis determined by the CI preprocessor as described in the previous step. The electron density of the ground state N-electron wave-function is sent to Sentaurus.
6. A script calls Sentaurus Device in a loop and adjusts a fictitious band gap narrowing parameter Δ_{bgn} at each grid point in the quantum region so that, the solved electron density in the quantum region will match that predicted by the CI.
7. Sentaurus outputs a new electrostatic potential (with the fictitious Δ_{bgn} removed) and electron density. These quantities are compared with the previous iteration's potential and density. If convergence has been reached, the process ends, otherwise we return to 3 above with the new electrostatic potential and electron density.

RESULTS / EXAMPLE

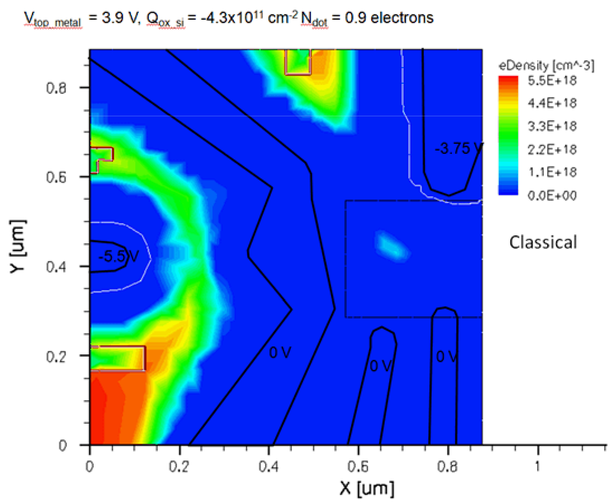

Figure 2. Classical Electron Density for Quantum Dot

Figure 2 shows the electron density of the left side of a double quantum dot structure. The polysilicon depletion gate outlines are shown. The accumulation gate is a blanket aluminum layer above the depletion gates separated from them by two dielectric layers. The gate biases are optimized to produce close to one electron, in this case 0.94 electrons.

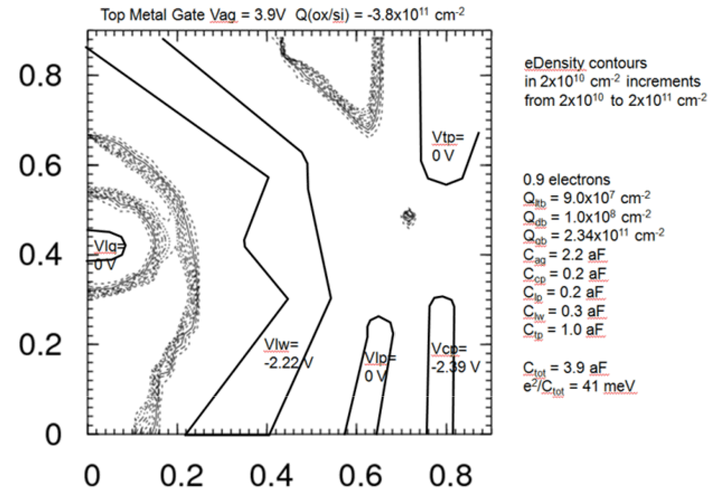

Figure 3. Electron Density of Quantum Dot after CI Solution.

The electron density after incorporating the CI solution in the quantum dot region is shown in Figure 3. Note that the lateral extent of the quantum dot charge is reduced compared to the classical result shown in Figure 1.

The electron density after incorporating the CI solution in the quantum dot region is shown in Figure 3. Note that the lateral extent of the quantum dot charge is reduced compared to the classical result shown in Figure 1.

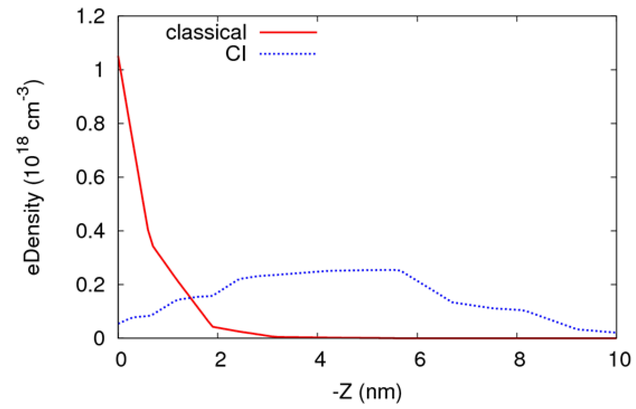

Figure 4. Electron Density along a Vertical Slice Showing the Classical and Quantum Mechanical (CI) Solutions.

A more dramatic difference between the classical and quantum solutions is seen along a vertical slice through the quantum dot. See Figure 4. This points out the significant adjustment needed using Δ_{bgn} in step 6.

The table below shows CI calculations of the ground state energy of dot occupations from 1 to 4 electrons for the structure shown in Figures 1-3. A basis set of 5 Gaussians is compared to a basis set of 9 Gaussians.

	5-Gaussians	9-Gaussians
1 electron	17.2	17.0
2 electrons	47.6	44.4
3 electrons	86.5	81.3
4 electrons	134.0	127.5

Sandia National Laboratories

This work was supported by the Laboratory Directed Research and Development program at Sandia National Laboratories. Sandia is a multi-program laboratory operated by Sandia Corporation, a Lockheed Martin Company, for the United States Department of Energy's National Nuclear Security Administration under Contract DE-AC04-94AL85000

LDRD LABORATORY DIRECTED RESEARCH & DEVELOPMENT